

## EXCITATION OF OSCILLATIONS IN PHOTOSPHERIC FLUX TUBES THROUGH BUFFETING BY EXTERNAL GRANULES

S. S. HASAN<sup>1,2</sup> AND W. KALKOFEN<sup>2</sup>

Received 1998 November 5; accepted 1999 February 15

### ABSTRACT

We examine the excitation of transverse (kink) and longitudinal (sausage) waves in magnetic flux tubes by granules in the solar photosphere. The investigation is motivated by the interpretation of network oscillations in terms of flux tube waves. We model the interaction between a granule, with a specified transverse velocity, and a vertical flux tube in terms of the Klein-Gordon equation, which we solve analytically as an initial value problem for both wave modes, assuming the same external impulse. The calculations show that for magnetic field strengths typical of the network, the energy flux in transverse waves is higher than in longitudinal waves by an order of magnitude, in agreement with the chromospheric power spectrum of network oscillations observed by Lites, Rutten, & Kalkofen. But for weaker fields, such as those that might be found in internetwork regions, the energy fluxes in the two modes are comparable. This result implies that if there are internetwork oscillations in magnetic flux tubes, they must show the cutoff periods of both longitudinal and transverse modes at 3 minutes and at 7 minutes or longer. We also find that granules with speeds of about  $2 \text{ km s}^{-1}$  can efficiently excite transverse oscillations in frequent short-duration (typically 1 minute) bursts that can heat the corona.

*Subject headings:* MHD — Sun: magnetic fields — Sun: oscillations

### 1. INTRODUCTION

It is well known from observations that the solar photosphere is threaded with strong (kilogauss) vertical magnetic fields in the form of flux tubes, which occur preferentially in the Ca network at the boundaries of supergranular cells on the disk (e.g., Stenflo 1994). These magnetic elements or flux tubes occur in intergranular lanes, where they are observed as small bright points (Dunn & Zirker 1973; Mehlretter 1974; Muller 1983, 1985; Muller et al. 1994; Berger et al. 1995) with diameters of typically 100 km. Observations with subarcsecond spatial resolution have revealed that these network bright points (NBPs) are in a highly dynamical state (Tarbell et al. 1989; Muller et al. 1992; Muller & Roudier 1992; Title et al. 1992; Muller et al. 1994; Berger et al. 1998; van Ballegooijen et al. 1998), exhibiting random motions with a broad velocity distribution. A histogram of NBP velocities by Muller et al. (1994), shows a mean speed of around  $1.5 \text{ km s}^{-1}$ , but they also find several instances when the velocities can intermittently become as high as  $3 \text{ km s}^{-1}$ . From an analysis of G band observations van Ballegooijen et al. (1998) found that the temporal variation of the bright point velocity had a correlation time of about 100 s. It is likely that the motions associated with NBPs can excite oscillations in magnetic flux tubes, which could contribute toward coronal heating.

Several observations have shown that the chromosphere in the magnetic network of the quiet Sun oscillates with a period of around 7 minutes (Damé 1983; Lites, Rutten, & Kalkofen 1993, hereafter LRK93; Curdt & Heinzel 1998). In order to analyze the oscillations and deduce the properties of the atmosphere, the nature of the waves and the origin of the periods must be known. A model of network bright points must explain the wave period and the heating. Furthermore, it must be compatible with the observational data regarding the power spectrum at the line center of the

Ca<sup>+</sup> H line (LRK93, Fig. 6) and the velocity phase coherence spectrum between the base of the chromosphere and the layer of formation of H<sub>3</sub> (LRK93, Fig. 7). The power spectrum shows a peak at 7 minutes, and the coherence spectrum shows very low coherence at all periods, implying that the waves giving rise to the Doppler motion at disk center do not come from below.

Two explanations have been proposed for the above oscillations: in terms of internal gravity waves forming standing waves in a chromospheric cavity (e.g., Deubner & Fleck 1990) and in terms of kink or transverse waves in magnetic flux tubes oscillating at their cutoff period (Kalkofen 1997; hereafter K97). For internal gravity waves, the wave period is determined by the temperature structure of the photosphere and chromosphere; for kink waves, the observed period is equal to the cutoff period, which depends on the temperature itself and on the strength of the magnetic field in the photosphere. The above idea by Deubner & Fleck in terms of gravity waves may explain the observed wave periods (Lou 1995a, 1995b) but fails to account for the heating of the chromosphere (K97). Transverse waves in the scenario of K97 can dissipate and heat the chromosphere, but only after conversion to longitudinal modes.

An alternative model that is consistent with the observational data is based on the excitation of kink tube waves generated in the photosphere through the impulse imparted by granules to magnetic flux tubes. The basis of this model is the observation of Muller et al. (1992, 1994) of intermittent, rapid motions of NBPs, which has been modeled by Choudhuri, Auffret, & Priest (1993, hereafter CAP93) and Choudhuri, Dikpati, & Banerjee (1993) as footpoint displacement of flux tubes, which results in upward-propagating transverse or kink waves. They reasoned that these waves could in principle carry sufficient energy to heat the corona. Other studies on the excitation of kink waves through periodic and turbulent footpoint motions in the convection zone have been undertaken by Ulmschneider, Zähringer, & Musielak (1991) and by Musielak et al. (1994), Huang, Musielak, & Ulmschneider (1995), Musielak et al.

<sup>1</sup> Indian Institute of Astrophysics, Bangalore 560034, India; hasan@iiap.ernet.in.

<sup>2</sup> Harvard-Smithsonian Center for Astrophysics, Cambridge, MA 02138.

(1995), and Zhugzhda, Bromm, & Ulmschneider (1995). The above investigations were carried out using a one-dimensional treatment based on the thin flux tube approximation. The generation of transverse waves through granular buffeting has also been found in the two-dimensional numerical simulations of Steiner et al. (1998). All these studies indicate that impulsive or turbulent footpoint motions can in principle excite sufficient energy in transverse waves for coronal heating. We should also mention that these effects are also present in three-dimensional numerical simulations of magnetoconvection (Nordlund & Stein 1989, 1990; Stein, Brandenburg, & Nordlund 1992; Nordlund et al. 1992).

A fundamental difficulty associated with the transverse wave scenario is that these waves are invisible at disk center. However, it should be borne in mind that, owing to the rapid decrease in density with height, the velocity amplitude  $v_{\perp}$  of upwardly propagating waves grows exponentially with height—as  $\exp(z/4H)$  in the isothermal limit (e.g., Spruit 1981), where  $H$  is the density scale height. In the chromosphere the velocity amplitude becomes comparable to the tube speed of kink waves leading to an efficient coupling of the transverse waves to longitudinal or sausage flux tube waves and consequently to a transfer of power to the latter. The longitudinal waves, which are compressive, can dissipate by forming shocks. Support for this hypothesis comes from the calculations by Zhugzhda et al. (1995; see also Ulmschneider et al. 1991), which is based on impulsive footpoint displacement analogous to that studied by CAP93.

The impulsive excitation of waves in a flux tube in general leads to the formation of a pulse that propagates away at the kink tube speed  $c_k$ , followed by a wake in which the flux tube oscillates at the cutoff period  $P_k$  of kink waves (cf. Spruit & Roberts 1983). This characteristic signature will be preserved even after the transformation of the transverse waves into longitudinal waves.

The aforementioned scenario of network bright point oscillations and heating is compatible with observations. As already noted, the transverse waves, generated in the photosphere, give a negligible contribution to the Doppler signal at disk center. However, in the chromosphere they are detected after transformation into longitudinal waves with the same period. The transfer of power between the modes takes place in the nonlinear regime and hence is very noisy. In addition, the longitudinal waves are excited by transverse waves whose cutoff period is much longer than that of the longitudinal waves. This corresponds to the long-period driving of acoustic waves (they are also described by the Klein-Gordon equation), which also results in a noisy wave spectrum (Kalkofen et al. 1994, Fig. 11). This noisy wave spectrum is consistent with the broad intensity maxima as a function of time shown by the Ca H line core (LRK93, Fig. 2). Furthermore, the value of the kink wave cutoff period, which depends on the strength of the magnetic field, is consistent with the observed magnetic field strength of magnetic flux tubes (Ruedi et al. 1992; Stenflo 1994).

The present investigation is based on an examination of the hypothesis, described above, of the excitation of transverse waves by the rapid motion of magnetic flux tubes, based on the observations by Muller et al. (1992, 1994) of rapid granular motion near photospheric bright points and modeled by CAP93. This model implicitly assumes that the velocities associated with bright points solely excite trans-

verse waves, whereas in principle there may also be slowly varying motions (with frequencies below the kink cutoff frequency) that do not efficiently generate transverse waves (van Ballegoijen et al. 1998). Furthermore, the observed motions may also lead to the generation of sausage oscillations, which represent an axisymmetric compression of the flux tube. Thus, it would be more appropriate to determine the motion of the network bright points as a response to granular buffeting by posing the question as an interaction problem and calculating the amplitude of the resulting transverse and longitudinal motions, in contrast to the approach adopted by CAP93 and Muller et al. (1994).

Our paper, based on the above hypothesis, examines the linear response of a vertical magnetic flux tube under the action of an impulse in the ambient medium. It should be noted that the linear interaction between a monochromatic acoustic wave or  $p$ -mode and a flux tube has been studied very extensively for an unstratified atmosphere (e.g., Ryutov & Ryutova 1976; Spruit 1982; Bogdan & Zweibel 1985; Zweibel & Bogdan 1986; Ryutova & Priest 1993; see also the reviews by Bogdan 1992, 1994, and references therein). Recently, the problem has been extended to include the effects of gravity by Bogdan et al. (1996) for a polytrope and by Hasan (1997) for an isothermal atmosphere. These papers essentially determined the coupling of  $p$ -modes with flux tube waves in the asymptotic time limit. The time-dependent interaction of a pulse in the external medium acting on a flux tube does not appear to have received adequate attention. We exclude treatments in which the problem involves the response of a tube to a specified motion of its footpoints or to a pressure perturbation at the base; rather we are concerned with the response of a tube under the driving action of a known force in the ambient medium.

Specifically, we examine the proposition that for intense flux tubes encountered in the magnetic network, the effect of an impulse delivered horizontally on the sides of the tube yields mainly transverse waves, and that for the weaker fields in the cell interior, a larger fraction of the wave flux appears in the form of longitudinal waves. We determine which modes are preferentially excited by calculating the partitioning of energy in the two wave modes, for the *same external impulse*. The theoretical results obtained in this paper support the inference drawn from chromospheric power spectra that the magnetic flux tubes show mainly transverse waves. For  $K_{2v}$  bright points our results, together with the absence of long-period oscillations from the cell interior chromosphere, imply that  $K_{2v}$  bright points are powered by pure acoustic waves and not by longitudinal magnetoacoustic waves. In addition we also examine the excitation of transverse waves due to footpoint motion to compare with the earlier work of CAP93.

The plan of the paper is as follows: in § 2 we present the linear wave equations for the interaction of transverse and longitudinal modes with an external impulse; the analytic solutions for kink and longitudinal wave modes along with expressions for the energy flux are given in § 3. We present results for some illustrative cases in § 4 and discuss their salient features in § 5. Finally, the main conclusions of the work are summarized in § 6.

## 2. EQUATIONS FOR A THIN FLUX TUBE

We consider a vertical magnetic flux tube extending through the photosphere. If the tube is sufficiently thin so

that radial variations can be neglected to leading order, the analysis is considerably simplified. We adopt this approximation for mathematical tractability and examine linear displacements of the flux tube, which are described by kink or transverse (Spruit 1981) and sausage or longitudinal waves (Roberts & Webb 1978). We also include the effect of perturbations in the external medium, since our aim is to study the excitation of tube oscillations due to the forcing action of granules. The relevant linear equations for both wave modes are well known and given in Appendix A for convenience.

Since we are primarily concerned in this paper with the photospheric layers of the flux tube, it is reasonable to assume that the atmosphere is isothermal. Although in the higher layers this assumption is not so good, we adopt it nonetheless for reasons of mathematical tractability. We work in terms of the “reduced” displacement  $Q(z, t)$  which is related to the physical Lagrangian displacement  $\xi(z, t)$  by

$$Q_{\kappa}(z, t) = \xi_{\perp}(z, t)e^{-z/4H}$$

for kink or transverse oscillations and by

$$Q_{\lambda}(z, t) = \xi_{\parallel}(z, t)e^{-z/4H}$$

for sausage or longitudinal oscillations, where  $H$  denotes the scale height of the atmosphere.

Starting from equations (A1) and (A11), it can be shown that the reduced displacement  $Q_{\alpha}$  ( $\alpha = \kappa$  for transverse waves and  $\alpha = \lambda$  for longitudinal waves) in an isothermal and magnetized medium satisfies the Klein-Gordon equation

$$\frac{\partial^2 Q_{\alpha}}{\partial z^2} - \frac{1}{c_{\alpha}^2} \frac{\partial^2 Q_{\alpha}}{\partial t^2} - k_{\alpha}^2 Q_{\alpha} = F_{\alpha}, \quad (1)$$

where  $k_{\alpha} = \omega_{\alpha}/c_{\alpha}$ ,  $\omega_{\alpha}$  is the cutoff frequency for the wave, and  $c_{\alpha}$  is the wave propagation speed in the medium. The speeds for the transverse and longitudinal waves are, respectively,

$$c_{\kappa}^2 = \frac{2}{\gamma} \frac{c_s^2}{1 + 2\beta},$$

$$c_{\lambda}^2 = \frac{c_s^2}{1 + \gamma\beta/2},$$

where  $c_s$  is the sound speed,  $\gamma$  is the ratio of specific heats ( $\gamma = 5/3$ ),  $\beta = 8\pi p/B^2$ ,  $p$  is the gas pressure inside the tube, and  $B$  is the magnitude of the vertical component of the magnetic field on the tube axis.

The cutoff frequencies for transverse and longitudinal waves are, respectively,

$$\omega_{\kappa}^2 = \frac{g}{8H} \frac{1}{1 + 2\beta}, \quad (2)$$

$$\omega_{\lambda}^2 = \omega_{\text{BV}}^2 + \frac{c_{\lambda}^2}{H^2} \left( \frac{3}{4} - \frac{1}{\gamma} \right)^2, \quad (3)$$

where  $\omega_{\text{BV}}^2 = g^2(\gamma - 1)/c_s^2$  is the Brunt-Väisälä frequency.

### 2.1. Form of the Forcing Functions

The forcing functions  $F_{\alpha}$  appearing in equation (1) are (see eq. [A4])

$$F_{\kappa}(z, t) = -e^{-z/4H} \frac{2(\beta + 1)}{2\beta + 1} \frac{1}{c_{\kappa}^2} \frac{\partial \mathcal{V}_{\perp,e}}{\partial t} \quad (4)$$

for the transverse wave, where  $\mathcal{V}_{\perp,e}(z, t)$  denotes the transverse component of the external granule velocity, and for the longitudinal wave (see eq. [A13])

$$F_{\lambda}(z, t) = e^{-z/4H} \frac{\beta + 1}{2p_e} \left( \frac{d}{dz} + \frac{1}{\gamma H} \right) \Pi_e, \quad (5)$$

where  $\Pi_e$  denotes the (Eulerian) perturbation in the external pressure and  $p_e$  is the external gas pressure.

The form of the granule velocity in the external medium needs to be specified. For simplicity we assume that the granules buffet the tube at a fixed level in the atmosphere corresponding to  $z = 0$ .

Let the external granule velocity have the form

$$\mathcal{V}_{\perp,e}(z, t) = V_{\perp,e} f(t) \delta(z/H), \quad (6)$$

where  $f(t)$  describes the time dependence of the impulse,  $V_{\perp,e}$  denotes the amplitude of the external velocity, and  $\delta$  is the Dirac  $\delta$  function.

Since our aim is to compare the wave energy in transverse and longitudinal oscillations we need to relate the granule velocity  $\mathcal{V}_{\perp,e}$  to the external pressure perturbation  $\Pi_e$ . We do this by using the linearized equation of motion in the field-free medium for the transverse component of the velocity, viz.,

$$\rho_e \frac{\partial \mathcal{V}_{\perp,e}}{\partial t} = - \frac{\partial \Pi_e}{\partial x}, \quad (7)$$

where  $\rho_e$  is the gas density in the surrounding atmosphere.

Integrating equation (7) with respect to  $x$ , we find

$$\Pi_e(z, x, t) - \Pi_e(z, x_0, t) = \rho_e \Delta x \left\langle \frac{\partial \mathcal{V}_{\perp,e}}{\partial t} \right\rangle,$$

where  $\langle \partial \mathcal{V}_{\perp,e} / \partial t \rangle$  denotes the average value of the acceleration  $\partial \mathcal{V}_{\perp,e} / \partial t$  in the interval  $\Delta x = x_0 - x$ . The latter is essentially the distance a granule travels in the horizontal direction before impinging on the tube. Dropping the angular brackets and assuming that  $\Pi_e = 0$  at  $x = x_0$  and that  $\Delta x$  is comparable to the pressure scale height, we have

$$\Pi_e \approx aH\rho_e \frac{\partial \mathcal{V}_{\perp,e}}{\partial t}, \quad (8)$$

where  $a$  is a factor of order unity.

### 3. SOLUTIONS OF THE LINEARIZED WAVE EQUATIONS

We now develop solutions for the “reduced” displacements that satisfy the Klein-Gordon equation (1), using standard techniques. For an infinite medium (i.e., extending from  $z = -\infty$  to  $z = +\infty$ ) the solution can be written conveniently as follows (Morse & Feshbach 1953):

$$Q_{\alpha}(z, t) = \int_0^t dt_0 \int_{-\infty}^{\infty} dz_0 F_{\alpha}(z_0, t_0) G_{\alpha}(z, z_0; t, t_0), \quad (9)$$

in terms of  $G$ , the Green’s function, given by

$$G_{\alpha}(z, z_0; t, t_0) = \frac{c_{\alpha}}{2} J_0 \left[ \omega_{\alpha} \sqrt{(t - t_0)^2 - \frac{(z - z_0)^2}{c_{\alpha}^2}} \right] \times \mathcal{H} \left( t - t_0 - \frac{|z - z_0|}{c_{\alpha}} \right), \quad (10)$$

where  $z$ ,  $t$  and  $z_0$ ,  $t_0$  denote, respectively, the field and source coordinates;  $J_0$  denotes the zeroth order Bessel function;  $\mathcal{H}$  is the Heaviside function; and  $\omega_{\alpha}$  is the cutoff

frequency of the wave. Note that we have implicitly assumed that  $Q_\alpha$  and  $\partial Q_\alpha/\partial t$  vanish at  $z = \pm\infty$ .

By substituting the functions  $F_\alpha$  given by equations (4) and (5), we can explicitly calculate the displacements  $Q_\alpha$  for the different wave modes.

### 3.1. Kink Waves

Substituting equations (4) and (10) in equation (9) and using equation (6) for the external velocity we find that the solution for the transverse displacement in a kink wave is given by

$$Q_\kappa(z, t) = -D_\kappa \int_0^{t-z/c_\kappa} dt_0 f'(t_0) J_0(\omega_\kappa \zeta_\kappa), \quad (11)$$

where

$$\zeta_\kappa = \sqrt{(t-t_0)^2 - (z/c_\kappa)^2},$$

and

$$D_\kappa = \frac{\beta+1}{2\beta+1} \frac{V_{\perp,e}}{c_\kappa} H.$$

In order to determine the reduced velocity  $\dot{Q}_\kappa$ , we differentiate equation (11) for the displacement with respect to  $t$  to obtain

$$\begin{aligned} \dot{Q}_\kappa(z, t) = & -D_\kappa \left[ f' \left( t - \frac{z}{c_\kappa} \right) - \int_0^{t-z/c_\kappa} dt_0 f'(t_0) \right. \\ & \left. \times \frac{\omega_\kappa(t-t_0)}{\zeta_\kappa} J_1(\omega_\kappa \zeta_\kappa) \right]. \end{aligned} \quad (12)$$

#### 3.1.1. Excitation of Kink Waves Due to Footpoint Motions

It is instructive to consider the solution of kink wave excitation when the footpoint motion is specified. Mathematically, this problem can be solved in terms of the velocity  $\dot{Q}_\kappa$  that satisfies the homogeneous form of the Klein-Gordon equation given by equation (1) for a semi-infinite medium, extending from  $z=0$  to  $z=\infty$ , and an inhomogeneous boundary condition at  $z=0$ , where  $\dot{Q}_\kappa(0, t)$  is specified as a function of time. The solution of this initial value problem in which  $\dot{Q}_\kappa(0, t) = 0$  for  $t < 0$  can once again be constructed using Green's function techniques and is (Doetsch 1956; see Appendix B for details)

$$\begin{aligned} \dot{Q}_\kappa(z, t) = & \left[ \dot{Q}_\kappa \left( 0, t - \frac{z}{c_\kappa} \right) \right. \\ & \left. - k_\kappa z \int_0^{t-z/c_\kappa} dt_0 \dot{Q}_\kappa(0, t_0) \frac{J_1(\omega_\kappa \zeta_\kappa)}{\zeta_\kappa} \right]. \end{aligned} \quad (13)$$

It can be shown that the above solution for the semi-infinite medium given by equation (13) is consistent with equation (12) for the infinite medium. This can be verified by calculating  $\dot{Q}_\kappa(0, t)$  (the footpoint velocity) from equation (12) for a specified form for the external granular velocity. When this solution is substituted in equation (13), the resulting velocity is identical to that found from equation (12). For purposes of comparison with CAP93 it is convenient to look at the Fourier representation of the above equation, which is

$$\dot{Q}_\kappa(z, t) = \int_0^t dt_0 \dot{Q}_\kappa(0, t_0) \int_{-\infty}^{\infty} d\omega e^{i[kz - \omega(t-t_0)]}, \quad (14)$$

where the wavenumber  $k$  and the frequency  $\omega$  are related by the dispersion relation,

$$\omega^2 = c_\kappa^2 k^2 + \omega_\kappa^2.$$

The above equation (eq. [14]) agrees with equation (10) used by CAP93 if we consider the initial time to be at  $t = -\infty$ .

#### 3.1.2. Wave Energy Flux in Kink Waves

We now calculate the vertical wave energy flux. The vertical component of the energy flux in transverse waves is given by (Bray & Loughhead 1974; see also Bogdan et al. 1996)

$$\mathcal{F}_\kappa = -\frac{B^2}{4\pi} \frac{\partial \xi_\perp}{\partial t} \frac{\partial \xi_\perp}{\partial z}. \quad (15)$$

In terms of the reduced displacement  $Q$  and velocity  $\dot{Q}$  we obtain (using the relation  $p/p_e = \beta/1 + \beta$ )

$$\mathcal{F}_\kappa = -\frac{2p_{e,0}}{\beta+1} \dot{Q}_\kappa \left( \frac{\partial Q_\kappa}{\partial z} + \frac{1}{4H} Q_\kappa \right) e^{-z/2H}, \quad (16)$$

where  $p_{e,0}$  is the gas pressure in the ambient medium at  $z=0$ . We find that the product of the energy flux and the cross section area of the tube  $A(z)$ , where  $A(z) = A(0)e^{z/2H}$  for an isothermal tube, does not have the exponential height dependence of the physical displacement.

We define the effective flux as

$$\mathcal{F}_{\kappa, \text{eff}} = n \mathcal{F}_\kappa A/A_\odot, \quad (17)$$

where  $n$  denotes the number of flux tubes on the Sun at  $z=0$  and  $A_\odot$  denotes the solar surface area. Hence  $nA/A_\odot$  is the fractional area on the Sun covered by magnetic flux tubes. The effective flux is then given by

$$\mathcal{F}_\kappa = -f_0 \frac{2p_{e,0}}{\beta+1} \dot{Q}_\kappa \left( \frac{\partial Q_\kappa}{\partial z} + \frac{1}{4H} Q_\kappa \right), \quad (18)$$

where  $f_0 = nA(0)/A_\odot$  is the filling factor at  $z=0$ .

### 3.2. Longitudinal Waves

The solution of the Klein-Gordon equation for the longitudinal displacement is

$$\begin{aligned} Q_\lambda(z, t) = & -D_\lambda \left\{ f' \left( t - \frac{z}{c_\lambda} \right) \right. \\ & + \int_0^{t-z/c_\lambda} dt_0 f'(t_0) \left[ \left( \frac{3}{4} - \frac{1}{\gamma} \right) \frac{c_\lambda}{H} J_0(\omega_\lambda \zeta_\lambda) \right. \\ & \left. \left. - \frac{k_\lambda z}{\zeta_\lambda} J_1(\omega_\lambda \zeta_\lambda) \right] \right\}, \end{aligned} \quad (19)$$

where

$$\zeta_\lambda = \sqrt{(t-t_0)^2 - (z/c_\lambda)^2},$$

and the external driving amplitude is

$$D_\lambda = \frac{\beta+1}{4} \frac{\gamma a}{c_s^2} V_{\perp,e}(0) H^2.$$

The solution for the velocity is

$$\begin{aligned} \dot{Q}_\lambda(z, t) = & -D_\lambda \left\{ f'' \left( t - \frac{z}{c_\lambda} \right) + f' \left( t - \frac{z}{c_\lambda} \right) \omega_\lambda \right. \\ & \times \left[ \left( \frac{3}{4} - \frac{1}{\gamma} \right) \frac{1}{k_\lambda H} - \frac{k_\lambda z}{2} \right] \\ & + \int_0^{t-z/c_\lambda} dt_0 f'(t_0) \omega_\lambda \frac{t-t_0}{\zeta_\lambda} \\ & \times \left[ \left( \frac{1}{\gamma} - \frac{3}{4} \right) \frac{c_\lambda}{H} J_1(\omega_\lambda \zeta_\lambda) \right. \\ & \left. \left. + \frac{k_\lambda z}{\zeta_\lambda} J_2(\omega_\lambda \zeta_\lambda) \right] \right\}. \end{aligned} \quad (20)$$

3.2.1. Wave Energy Flux in Longitudinal Waves

The vertical longitudinal energy flux in a thin flux tube is (Hasan 1997)

$$\begin{aligned} \mathcal{F}_\lambda = & \delta p V_z \\ = & \frac{\beta}{(\beta + 1)(2 + \gamma\beta)} p_e(0) \\ & \times \left[ \gamma(\beta + 1) \frac{\Pi_e}{p_e} - 2\gamma \frac{\partial \xi_\parallel}{\partial z} + \frac{2 - \gamma}{H} \xi_\parallel \right] \frac{\partial \xi_\parallel}{\partial t}. \end{aligned} \quad (21)$$

In terms of the reduced displacement  $Q_\lambda$  and velocity  $\dot{Q}_\lambda$ , the longitudinal flux (for  $z \neq 0$ ) is given by

$$\begin{aligned} \mathcal{F}_\lambda = & \frac{\beta}{(\beta + 1)(2 + \gamma\beta)} p_e(0) \dot{Q}_\lambda \\ & \times \left[ -2\gamma \frac{\partial Q_\lambda}{\partial z} + \left( 2 - \frac{3\gamma}{2} \right) \frac{Q_\lambda}{H} \right] e^{-z/2H}, \end{aligned} \quad (22)$$

and the effective longitudinal flux is

$$\begin{aligned} \mathcal{F}_{\lambda, \text{eff}} = & f_0 \frac{\beta}{(\beta + 1)(2 + \gamma\beta)} p_e(0) \dot{Q}_\lambda \\ & \times \left[ -2\gamma \frac{\partial Q_\lambda}{\partial z} + \left( 2 - \frac{3\gamma}{2} \right) \frac{Q_\lambda}{H} \right]. \end{aligned} \quad (23)$$

Once again the effective flux does not have the exponential  $z$  dependence associated with the physical displacement.

4. RESULTS

We now consider the explicit evaluation of  $Q$ ,  $\dot{Q}$ , and  $\mathcal{F}$  for the different modes when the external granule velocity is specified. For the time dependence, which enters through the function  $f(t)$ , we follow CAP93 and take the form

$$f(t) = e^{-(t/\tau)^2}, \quad (24)$$

where  $\tau$  denotes the interaction time between a granule and the flux tube. This is related to the time  $T_f$  defined by CAP93 for the footpoint motion through the relation  $T_f = \pi^{1/2}\tau$ .

We choose a value of the pressure ratio  $\beta$  that is representative for the solar photosphere. From observations and empirical modeling (e.g., Rüedi et al. 1992; Kneer, Hasan, & Kalkofen 1996; Hasan, Kneer, & Kalkofen 1998; and Kalkofen 1997) a value of the magnetic field strength corresponding to  $\beta = 0.3$  (which is constant with  $z$ ) appears

appropriate. Taking a temperature of  $T = 6650$  K, which corresponds to a scale height  $H = 155.4$  km and a sound speed of  $8.4$  km s<sup>-1</sup>, the transverse and longitudinal wave speeds are  $c_\kappa = 7.3$  km s<sup>-1</sup> and  $c_\lambda = 7.5$  km s<sup>-1</sup>, respectively. When  $\beta = 0.3$  the longitudinal waves have a slightly larger phase speed than the transverse waves. For the external granule we choose  $V_{\perp, e} = 1$  km s<sup>-1</sup> and an interaction time of  $\tau = 50$  s. The results can easily be scaled to different values of  $V_{\perp, e}$  since this parameter enters linearly in the expressions for  $Q$  and  $\dot{Q}$  and quadratically in the effective flux. We use the above values as the default parameters, although we shall also study the effect of varying  $\beta$  and  $\tau$ .

Figure 1 shows the variation with time of the transverse (solid lines) and longitudinal (dotted lines) reduced velocities  $\dot{Q}$  in the flux tube at two different heights ( $z = 500$  km and  $z = 1250$  km), using the default parameters. It should be noted that  $\dot{Q}$  needs to be scaled by the factor  $\exp(z/4H)$  to determine the true velocity. Consequently, the actual velocity at  $z = 1250$  km is a factor of about 3.3 larger than the velocity at  $z = 500$  km. The external impulse imparted by the granule to the flux tube at  $z = 0$ , starting at  $t = 0$ , generates a wave that propagates away in both directions. We consider solely the upward-propagating pulse, which travels with the phase speed  $c_\alpha$  ( $\alpha = \kappa$  or  $\lambda$ ) and arrives at a height  $z$  after a time  $z/c_\alpha$ . The first maximum in  $\dot{Q}$  for the two modes is associated with the impulse due to the buffeting action of granules. This impulse arrives earlier for longitudinal waves than for transverse waves (for  $\beta = 0.3$ ) since the former have a slightly higher phase speed. After the passage of the primary impulse, the atmosphere oscillates as a whole with a single frequency. An inspection of Figure 1 reveals that the period of the oscillation is in fact the cutoff period associated with the wave. From equations (2) and (3), the cutoff periods for the kink and longitudinal waves are, respectively (assuming  $\gamma = 5/3$ ),

$$P_\kappa = P_a \sqrt{2\gamma(1 + 2\beta)}, \quad (25)$$

and

$$P_\lambda = P_a \sqrt{(60 + 50\beta)/(63 + 48\beta)}, \quad (26)$$

where  $P_a = c_s/2H$  is the acoustic cutoff frequency of an unmagnetized isothermal atmosphere. For a sound speed of

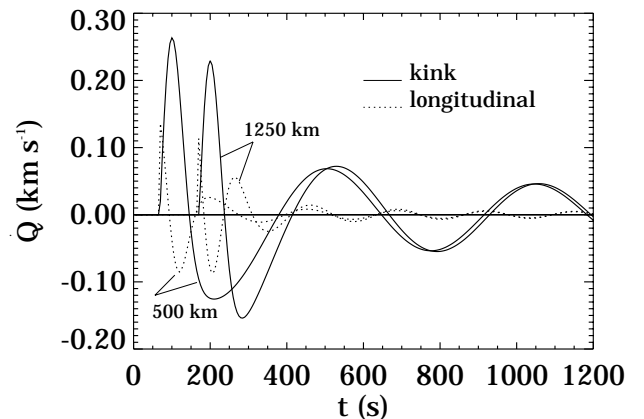


FIG. 1.—Variation with time of the transverse (solid lines) and longitudinal (dotted lines) reduced velocity  $\dot{Q}$  in the flux tube at two different heights ( $z = 500$  km and  $z = 1250$  km) for  $\beta = 0.3$  (where  $\beta$  is the ratio of gas to magnetic pressure), an interaction time  $\tau = 50$  s, and horizontal granular speed  $V_{\perp, e} = 1$  km s<sup>-1</sup>. Note that  $\dot{Q}$  needs to be scaled by  $\exp(z/4H)$  to determine the actual velocity.

$c_s = 8.4 \text{ km s}^{-1}$ , the cutoff periods are  $P_a = 231 \text{ s}$ ,  $P_\kappa = 534 \text{ s}$ , and  $P_\lambda = 227 \text{ s}$ . Note that the cutoff period of the longitudinal wave is practically the same as that of a sound wave in an unmagnetized medium. We also find that the amplitude of the primary peak is about twice as large for kink waves as for longitudinal waves.

Figure 2 shows the time variation of the wave energy flux in the vertical direction,  $F_{\text{wave}}/f_0$  (where  $f_0$  denotes the filling factor of magnetic flux tubes at  $z = 0$ ), in transverse (solid lines) and longitudinal (dotted line) modes at two different heights, using the default parameters. Note that the energy flux in longitudinal waves is measured by the scale on the right. The time behavior is similar to that in the previous figure. The impulse delivered to the tube at  $z = 0$  creates an oscillation that transports energy to the higher layers.

The vertical energy flux in transverse waves is about 15 times larger than the energy flux in longitudinal waves. In order to understand this behavior, consider the solutions in the limit  $\beta \ll 1$ , when we find from equations (11) and (12) that  $Q_\kappa \sim Q_\lambda$ . From equations (16) and (23) we see that  $F_{\lambda,\text{eff}}/F_{\kappa,\text{eff}} \sim \beta$ , which shows that for small values of  $\beta$ , the longitudinal energy flux is much smaller than the energy flux in transverse waves. From Figure 1, the ratio of velocities in the primary pulse is  $\dot{Q}_\kappa/\dot{Q}_\lambda \approx 2$ , and the ratio of the

displacements is approximately the same. For  $\beta = 0.3$ , we thus find  $F_{\kappa,\text{eff}}/F_{\lambda,\text{eff}} \sim 4/0.3 = 13.3$ , which is in good agreement with the value seen in Figure 2.

We now examine the effect of varying  $\beta$  on the velocity of the transverse and longitudinal waves. Figure 3a shows the time variation of the transverse velocity  $\dot{Q}_\kappa$  in the flux tube at  $z = 500 \text{ km}$  for various values of  $\beta$ . The first maximum of  $\dot{Q}_\kappa$ , associated with the initial impulse, increases gradually with  $\beta$ , although the amplitude of the subsequent maxima and minima exhibit little variation. The reason for the slow increase is evident from equations (11) and (12), which show that  $Q_\kappa \sim \dot{Q}_\kappa \sim \beta^{1/2}$  when  $\beta \gg 1$ . The period of the oscillation after the passage of the primary pulse is the cutoff period  $P_\kappa$ , and from the figure we find that  $P_\kappa$  increases with  $\beta$ . This can be seen from equation (25), which yields  $P_\kappa \sim \beta$ , when  $\beta \gg 1$ .

Figure 3b depicts the time variation of the longitudinal velocity  $\dot{Q}_\lambda$  in the flux tube at  $z = 500 \text{ km}$  for various values of  $\beta$ . The maximum of  $\dot{Q}_\lambda$ , associated with the initial impulse, increases with  $\beta$ . In contrast to the case of kink waves,  $\dot{Q}_\lambda$  increases more rapidly with  $\beta$ . From equation (20) we find that in the limit  $\beta \gg 1$ ,  $\dot{Q}_\lambda \sim \beta$ . The period of the oscillation after the passage of the initial impulse, however, does not vary with  $\beta$  in view of the fact that the longitudinal cutoff period  $P_\lambda$ , given by equation (26), is practically independent of  $\beta$ .

Figure 4a shows the time variation of the vertical energy flux in transverse waves  $F_\kappa/f_0$  at  $z = 500 \text{ km}$  for various values of  $\beta$  (where  $f_0$  is the magnetic filling factor at  $z = 0$ ). We find that the maximum value of the flux associated with the primary pulse increases gradually with  $\beta$ . For  $\beta \gg 1$  we have already shown that  $Q_\kappa$  (and  $\dot{Q}_\kappa$ )  $\sim \beta^{1/2}$ , whereas  $\partial Q_\kappa/\partial z \sim Q_\kappa/c_\kappa \sim \beta$  (noting that  $c_\kappa \sim 1/\beta^{1/2}$  when  $\beta \gg 1$ ). Therefore, from equation (18), we find that for  $\beta \gg 1$

$$F_{\kappa,\text{eff}} \sim \frac{1}{\beta} \beta \sqrt{\beta} \sim \sqrt{\beta}.$$

Figure 4b shows the variation with time of  $F_\lambda/f_0$ , the vertical energy flux in longitudinal waves at  $z = 500 \text{ km}$  for various values of  $\beta$ . The primary maximum in the flux (associated with the initial impulse) increases sharply with  $\beta$ . The rapid increase of  $F_\lambda$  with  $\beta$  can be understood from equation (23). Noting that  $\partial Q_\lambda/\partial z \sim Q_\lambda/c_\lambda \sim \beta^{3/2}$  for  $\beta \gg 1$ , we find that in this limit the longitudinal flux behaves

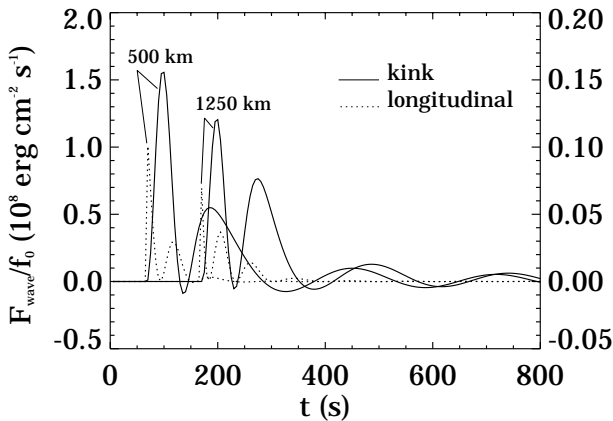


FIG. 2.—Variation with time of the wave energy flux in the vertical direction  $F_{\text{wave}}/f_0$  (where  $f_0$  denotes the filling factor of magnetic flux tubes at  $z = 0$ ) in transverse (solid lines) and longitudinal (dotted line) modes at two different heights ( $z = 500 \text{ km}$  and  $z = 1250 \text{ km}$ ) for  $\beta = 0.3$ .

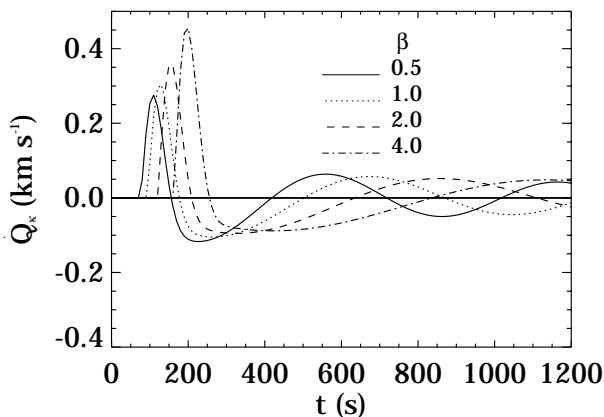


FIG. 3a

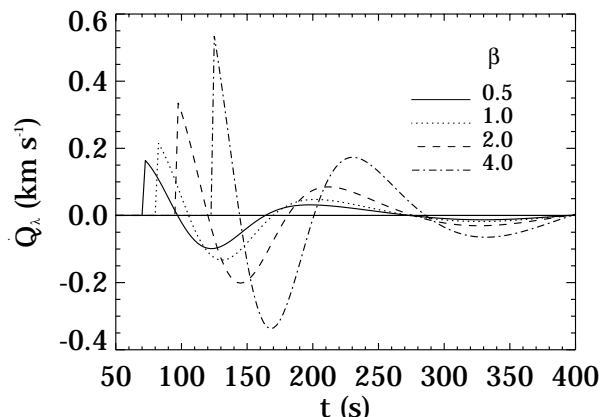


FIG. 3b

FIG. 3.—Variation with time of the (a) reduced transverse velocity  $\dot{Q}_\kappa$  and (b) reduced longitudinal velocity  $\dot{Q}_\lambda$  in the flux tube at  $z = 500 \text{ km}$  for various values of  $\beta$ , assuming an interaction time  $\tau = 50 \text{ s}$  and horizontal granule speed  $V_{1,e} = 1 \text{ km s}^{-1}$ .

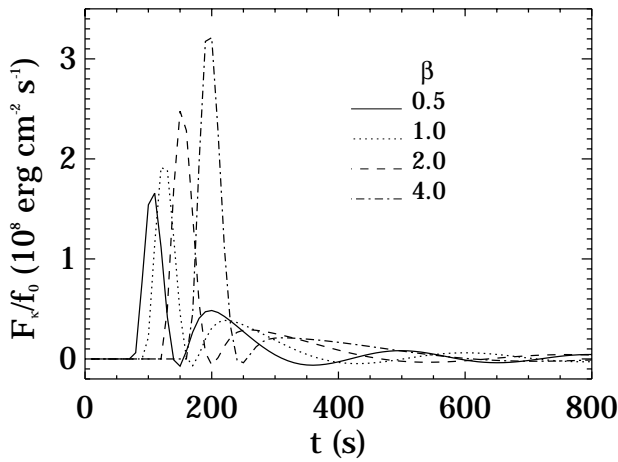


FIG. 4a

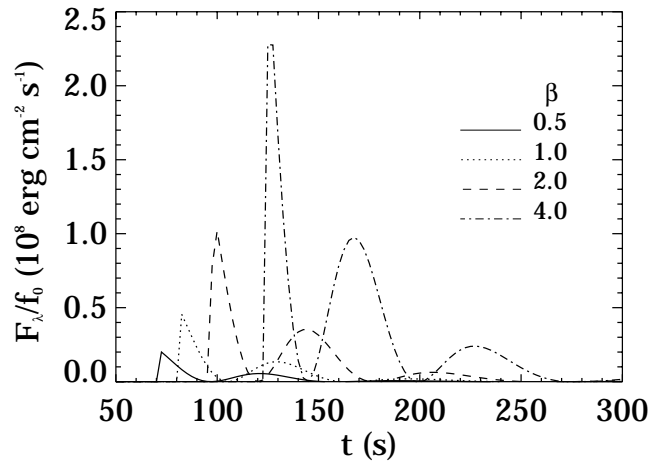


FIG. 4b

FIG. 4.—Variation with time of the (a) vertical transverse energy flux  $F_{\kappa}/f_0$  and (b) vertical longitudinal energy flux  $F_{\lambda}/f_0$  at  $z = 500$  km for various values of  $\beta$ , assuming an interaction time of  $\tau = 50$  s and a horizontal granule speed of  $V_{\perp,e} = 1$  km s $^{-1}$ .

approximately as

$$F_{\lambda,\text{eff}} \sim \beta^{3/2}.$$

For  $\beta \geq 2.0$ , the energy flux in longitudinal waves becomes comparable to that in transverse waves.

We now examine the consequence of varying the interaction time  $\tau$  between an external granule and the flux tube. To illustrate this, we treat only the case of transverse waves. Figure 5 shows the variation with time of  $Q_{\kappa}$ , the transverse displacement, at  $z = 500$  km for various values of  $\tau$ . We again find the general behavior discussed earlier, viz., the arrival of the impulse generated at  $z = 0$  followed by an oscillation at the kink wave cutoff period. The amplitude of the oscillation decreases with increasing  $\tau$ , but as noted earlier, the period of the oscillation is the same. For  $\omega_{\kappa}\tau \ll 1$  we find from equation (11) that  $Q_{\kappa}$  is practically independent of  $\tau$ , whereas for  $\omega_{\kappa}\tau \gg 1$ ,  $Q_{\kappa} \sim 1/\tau$ . On the other hand, the velocity  $\dot{Q}_{\kappa}$  associated with the primary pulse is essentially given by the first term in equation (12), so that  $\dot{Q}_{\kappa} \sim 1/\tau$ . Similarly,  $\partial Q_{\kappa}/\partial z \sim 1/\tau$ . Thus, from equation (16),  $F_{\kappa} \sim 1/\tau^2$  for small values of  $\tau$ . The rapid decrease of the peak value of the flux can be seen in Figure 6, which shows

the time variation of  $F_{\kappa}/f_0$ , the vertical energy flux in transverse waves, at  $z = 500$  km for various values of  $\tau$ .

It is of some interest to consider the situation when the footpoint motion of the flux tube is the same as that of the granules. This is the approach adopted by CAP93. Figure 7 shows the variation with time of  $Q_{\kappa}$ , the transverse displacement, at  $z = 500$  km for various values of  $\tau$  when the footpoint motion is specified as follows:

$$Q(0, t) = Q_0 f(t) \mathcal{H}(t), \tag{27}$$

where  $Q_0$  is chosen such that the total displacement of the footpoint is the same as that of a granule. We normalize  $Q_0$  with respect to the distance traveled by a granule, with an interaction time  $\tau = 50$  s and a speed  $V_{\perp,e} = 1$  km s $^{-1}$ . For small values of  $\tau$  (i.e., when  $\omega_{\kappa}\tau \ll 1$ ), the displacement shows a peak followed by an oscillation, with an amplitude that decreases in time. As  $\tau$  increases, the kink in the displacement decreases. For large times, the tube is displaced from its original equilibrium position to a final position that is independent of  $\tau$ . Also, when  $\tau$  is comparable or greater than the cutoff period, there is essentially no kink, but the whole tube is slowly displaced instead from its initial location at all heights. This result is in agreement with the one

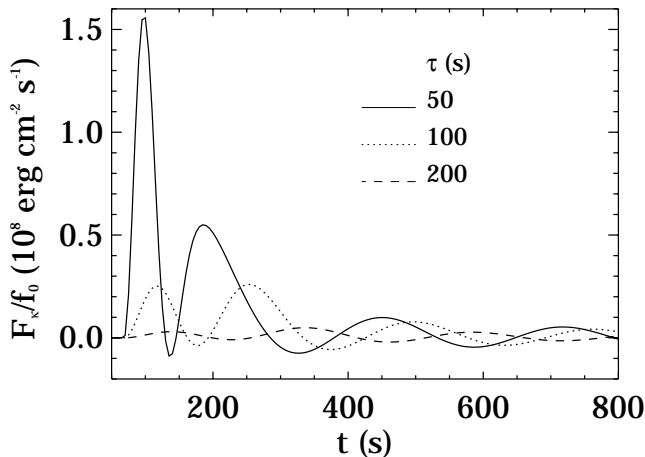


FIG. 5.—Variation with time of  $F_{\kappa}/f_0$ , the vertical energy flux in transverse waves, at  $z = 500$  km for various values of the interaction time  $\tau$  and a horizontal granule speed  $V_{\perp,e} = 1$  km s $^{-1}$ .

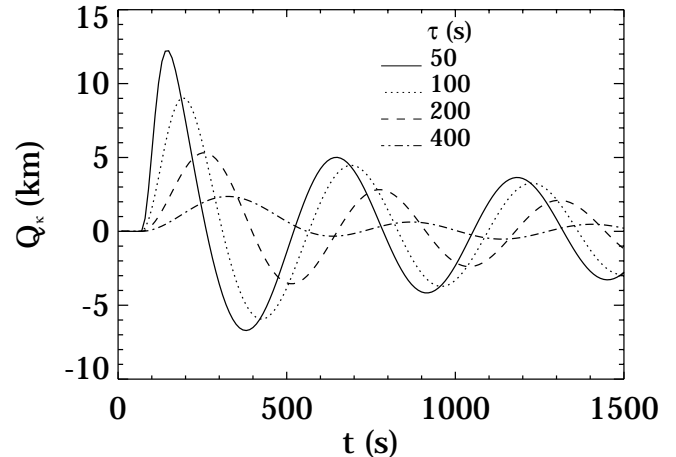


FIG. 6.—Variation with time of  $Q_{\kappa}$ , the transverse displacement, at  $z = 500$  km for various values of  $\tau$  and a horizontal granule speed  $V_{\perp,e} = 1$  km s $^{-1}$ .

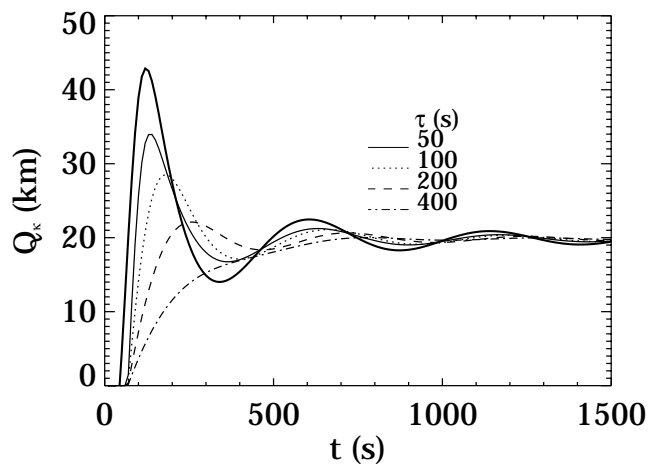


FIG. 7.—Variation with time of  $Q_k$ , the transverse displacement at  $z = 500$  km for various values of  $\tau$ , when the footpoint motion of the flux tube is specified according to eq. (27).

given by CAP93. We also find that the regimes where waves are excited or where a flux tube is merely displaced are separated by an interaction time of the order of half the cutoff period. Our integral expression for  $\dot{Q}$  (see eq. [13]) shows this clearly, as can be seen by replacing the Bessel function by a sine function, which is its asymptotic approximation and also a fair approximation everywhere.

In contrast, when the footpoint motion of the tube is determined from the granular motion through equation (1) we find that for all values of  $\tau$  the tube oscillates about its equilibrium position. The main difference is that when  $\tau$  becomes large, the peak value of the displacement becomes negligibly small.

## 5. DISCUSSION

We have examined the generation of waves in vertical flux tubes in the magnetic network through the impulsive excitation by granules. Our treatment has included both transverse and longitudinal waves. The generic behavior is the same for both waves: the buffeting action of a granule on a flux tube at a certain level excites a pulse that travels away from the source region with the kink or longitudinal tube speed. After the passage of the pulse, the atmosphere oscillates at the cutoff period of the mode, with an amplitude that slowly decays in time. The initial pulse carries most of the energy—subsequently the atmosphere oscillates as a whole in phase, without energy transport. We interpret the wave period observed in the magnetic network as the cutoff period of transverse waves, which leads naturally to an oscillation at this period (typically in the 7 minute range).

Our results indicate that the velocities in transverse and longitudinal waves excited by granules in the photosphere are comparable in magnitude for values of  $\beta$  that are typical of the magnetic network (i.e., when  $\beta \ll 1$ ). However, the vertical energy flux in transverse waves is an order of magnitude larger than that in longitudinal waves for network field strengths. The energy flux increases more rapidly with  $\beta$  for longitudinal waves than for transverse waves, and the fluxes are comparable for  $\beta \geq 2$ . Furthermore, the displacements  $Q$  and velocities  $\dot{Q}$  scale linearly and the energy fluxes  $F$  scale quadratically with the applied external velocity.

The analytic results for the energy flux generated by an impulse show that, for strong magnetic fields, most of the

energy goes into transverse waves and only a much smaller fraction into longitudinal waves. Physically, this appears reasonable as it is harder to excite sausage waves for small values of  $\beta$  since the compression of the flux tube is resisted by the strong magnetic field. Transverse waves, on the other hand, are incompressible and are therefore much less affected when the value of  $\beta$  becomes small. Observationally, our finding is consistent with the interpretation of network bright points in terms of flux tube waves, where the power spectrum observed in  $H_3$  by LRK93 shows a high peak at 2.5 mHz, presumably the cutoff frequency of kink waves, and a much smaller peak at 3 mHz, perhaps a contribution made by longitudinal flux tube waves. Our calculations therefore support the model of network bright points by K97 in which mainly transverse flux tube waves are excited and where the observed velocity signal measures the cutoff period of the transverse waves in the photosphere.

For weaker magnetic fields, such as those measured by Keller et al. (1994), we find the energy fluxes in the two modes to become comparable. From the absence of a strong peak at low frequencies in the power spectrum of the cell interior (CI) we conclude that both transverse and longitudinal waves must make a negligible contribution to  $K_{2\nu}$  bright point oscillations. The absence of the magnetic modes then implies that the waves in the CI are probably acoustic waves, and the observed 3 minute period is therefore the acoustic cutoff period, and not the cutoff period of longitudinal flux tube waves. From this we infer that the magnetic field structure in the CI is likely to be different from that of flux tubes in the magnetic network. One possibility is that if magnetic fields are associated with  $K_{2\nu}$  bright points, as suggested by Sivaraman & Livingston (1982), Kalkofen (1996), and Nindos & Zirin (1998), these fields may have the mixed polarity observed by Wang et al. (1995).

As regards the heating of the corona in coronal holes by kink waves, Muller et al. (1994) have estimated the energy flux generated by rapid footpoint motion ( $> 2$  km s $^{-1}$ ) of magnetic flux tubes based on the CAP93 calculations. Their estimate exceeds the coronal heating requirements (about  $3 \times 10^5$  ergs cm $^{-2}$  s $^{-1}$ ) by a modest factor of about 7. Such a small excess requires an  $e$ -folding distance for dissipating the energy that is a factor of 3 longer than the density scale height required for weak shocks (Ulmschneider 1970); the observations allow a scale length of 4 times the scale height (Withbroe 1988). However, Muller et al. (1994) have overestimated the energy flux for two reasons. First, they have used Spruit's (1981) value of the cutoff frequency  $\omega_k = 0.009$  s $^{-1}$  (corresponding to a period  $P_k = 700$  s), which is about twice as large as the value inferred from the oscillations in network bright points. For a more realistic cutoff period of around 450 s, the energy flux is further reduced. Second, as already mentioned in § 1, the assumption that motion of network bright points exclusively excites transverse waves is also questionable. This raises some doubts as to whether footpoint displacements can provide enough energy to heat the quiet corona. Our calculations based on more realistic parameters for the network yield an energy flux of

$$F_k = 1.5 \times 10^6 \left( \frac{v_0}{1 \text{ km s}^{-1}} \right)^2 \text{ ergs cm}^{-2} \text{ s}^{-1},$$

(see Fig. 5), for a filling factor of 0.01 and an interaction time of 50 s. For  $v_0 = 2$  km s $^{-1}$ , we get a flux that is about a



factor 20 higher than that needed to balance the energy losses of the quiet corona. Thus, kink waves generated in the photosphere may still provide a viable mechanism for coronal heating, provided the interaction time is much shorter than the cutoff period. Furthermore, for the process to be efficient, the transport of energy must essentially occur in frequent short-duration bursts. When the interaction time becomes large, the energy flux in transverse waves drops sharply (see Fig. 5) and the proposition that kink waves heat the quiet corona becomes less plausible.

## 6. SUMMARY AND CONCLUSIONS

We have developed a model for analyzing the excitation of transverse and longitudinal waves in a thin vertical flux tube through the buffeting action of a granule. Our treatment does not assume at the outset that the motions of the flux tube generate only transverse waves. Rather, we determine the response of the tube to the same initial impulse through a solution of the forced Klein-Gordon equation. We find that transverse waves are more efficiently excited than longitudinal waves in the magnetic network. For magnetic field strengths of the order of 1500 G, the energy flux in transverse waves is an order of magnitude larger than in longitudinal waves. Our results therefore support the conjecture of K97 that granular motions excite almost exclusively transverse waves in magnetic flux tubes. However, for weaker magnetic fields, the fluxes in the two modes become comparable. But we note that even though longitudinal waves gain in relative importance when the magnetic field becomes weak ( $\beta \gtrsim 2$ ), transverse waves are still excited and are detectable by their cutoff period ( $P \gtrsim 7$  minutes) in a power spectrum. Therefore, the absence of long-period oscillations in the so-called persistent flasher described by Brandt et al. (1992) implies that the 3 minute oscillations observed in these  $K_{2v}$  bright point must be caused by acoustic waves, and not by longitudinal flux tube waves.

The impulsive excitation leads to a disturbance traveling upward with the tube speed of transverse waves, and it is followed by a wake at the cutoff period with very high phase velocity (in the limit of  $t \rightarrow \infty$ , with infinite phase velocity). It is interesting to point out that the high-phase velocity of the oscillation in the wake of the initial pulse (which travels with the tube speed) is a straightforward property of impulsive solutions of the Klein-Gordon equation. High-phase velocities are therefore found also for longitudinal flux tube waves, as well as for the acoustic waves observed in  $K_{2v}$  bright points, where they may leave the erroneous impression that the high velocities indicate standing waves in a so-called chromospheric cavity. Furthermore, it should be noted that the initial pulse carries most of the energy. In the

subsequent oscillations of the atmosphere, the separation in time of the velocity maxima approaches the (corresponding) cutoff period, and velocity and pressure variation are related by a phase shift approaching  $90^\circ$ , i.e., the oscillation carries no energy (in the linear limit).

We find that granules with velocities of  $2 \text{ km s}^{-1}$  can contribute significantly to the generation of transverse energy flux in the magnetic network. This value is close to the mean value found from the histogram of NBP velocities deduced from observations (Muller et al. 1994). Efficient heating, however, requires that transverse waves be excited through frequent impacts of short duration (typically about 1 minute). Existing observations do not rule out this possibility. However, it would be desirable to have more observations that can provide information on the correlation time of the velocity in bright points. An observation that would support our scenario of network bright points would measure the expected polarization of the kink waves. Whereas the oscillations in the photosphere should not detect any Doppler motion at disk center, the transverse nature of the waves should become visible toward the limb of the Sun. We should stress that the aim of the present work was to examine the problem of wave excitation (transverse and longitudinal) in flux tubes and *not* to address the problem of coronal heating. The latter requires a nonlinear treatment, particularly in the higher layers of the atmosphere where the velocity amplitude of the waves becomes comparable to the kink or tube speed. In such regions, shock formation occurs and transverse waves can dissipate their energy through conversion to longitudinal waves (e.g., Ulmschneider et al. 1991; Huang et al. 1995; Zhugzhda et al. 1995). Another factor that has not been considered by us is the effect of wave reflection that would occur in the realistic case when the height variation of the wave speeds is taken into account. We should also mention that the use of the thin flux tube approximation becomes highly suspect in the chromosphere and above, where the radius of the flux tubes becomes larger than the local pressure scale height. The above refinements, as well as the influence of neighboring flux tubes, need to be considered in developing a model for wave heating of the corona. We hope to take account of some of these factors in future studies.

We acknowledge support from the National Science Foundation and NASA. S. S. H. is thankful to the Smithsonian Institution for travel support under SMIN grant 9411FR00007. We are grateful to A. R. Choudhuri for reading the manuscript and providing comments. We thank R. Muller for several useful discussions.

## APPENDIX A

### LINEAR EQUATIONS

#### A1. KINK WAVES

Following Spruit (1981), Ryutova & Priest (1993), and Bogdan et al. (1996), the linear equation for the transverse displacement  $\xi_\perp$  associated with a kink wave in a vertical thin flux tube to leading order is (neglecting the presence of steady flows in the ambient atmosphere)

$$\rho \frac{\partial^2 \xi_\perp}{\partial t^2} = g(\rho - \rho_e) \frac{\partial \xi_\perp}{\partial z} + \frac{B^2}{4\pi} \frac{\partial^2 \xi_\perp}{\partial z^2} + \rho_e \left( 2 \frac{\partial^2 \xi_{\perp,e}}{\partial t^2} - \frac{\partial^2 \xi_\perp}{\partial t^2} \right), \quad (\text{A1})$$

where  $\rho_e$  and  $\xi_{\perp,e}$  denote, respectively, the density and displacement in the external medium. The terms on the right-hand side denote the contributions by buoyancy, magnetic tension, and the force due to the external motions. Noting that  $\rho/\rho_e = \beta/(1 + \beta)$ , where  $\beta = 8\pi p/B^2$ ,  $p$  denotes the gas pressure inside the tube, and  $B$  is the vertical component of the magnetic field on the tube axis, equation (A1) can be rewritten as

$$\frac{\partial^2 \xi_{\perp}}{\partial t^2} + \frac{g}{2\beta + 1} \frac{\partial \xi_{\perp}}{\partial z} - \frac{2}{\gamma} \frac{c_s^2}{2\beta + 1} \frac{\partial^2 \xi_{\perp}}{\partial z^2} = 2 \frac{\beta + 1}{2\beta + 1} \frac{\partial^2 \xi_{\perp,e}}{\partial t^2}, \quad (\text{A2})$$

where  $c_s$  is the sound speed (constant by definition). We now define a new variable  $Q_{\kappa}$  as

$$\xi_{\perp} = e^{z/4H} Q_{\kappa}. \quad (\text{A3})$$

Making the above substitution in equation (A2) we obtain

$$\frac{\partial^2 Q_{\kappa}}{\partial z^2} - \frac{1}{c_{\kappa}^2} \frac{\partial^2 Q_{\kappa}}{\partial t^2} - k_{\kappa}^2 Q_{\kappa} = -e^{-z/4H} \frac{2(\beta + 1)}{2\beta + 1} \frac{1}{c_{\kappa}^2} \frac{\partial V_{\perp,e}}{\partial t}, \quad (\text{A4})$$

where

$$k_{\kappa}^2 = \frac{1}{16H^2}, \quad c_{\kappa} = \frac{2}{\gamma} \frac{c_s^2}{2\beta + 1}.$$

## A2. SAUSAGE WAVES

We start from the linearized equations for the sausage mode in a thin flux tube (Roberts & Webb 1978). In terms of the longitudinal displacement  $\xi_{\parallel} = \partial v_{\parallel}/\partial t$ , where  $v_{\parallel}$  is the vertical velocity, the relevant equations for sausage waves are

$$B \left[ \delta\rho + \frac{\partial}{\partial z} (\rho \xi_{\parallel}) \right] - \rho (\delta B_{\parallel} + B' \xi_{\parallel}) = 0, \quad (\text{A5})$$

$$\rho \frac{\partial^2 \xi_{\parallel}}{\partial z^2} + g \delta\rho + \frac{\partial \delta p}{\partial z} = 0, \quad (\text{A6})$$

$$\delta p + p' \xi_{\parallel} - c_s^2 (\delta\rho + \rho' \xi_{\parallel}) = 0, \quad (\text{A7})$$

$$\delta p + \frac{B \delta B_{\parallel}}{4\pi} = \Pi_e, \quad (\text{A8})$$

where  $\delta\rho$ ,  $\delta p$ , and  $\delta B_{\parallel}$  denote the Eulerian perturbations in density, pressure, and vertical magnetic field, respectively;  $\Pi_e$  is the Eulerian perturbation in the external pressure; and the prime symbol denotes a differential (e.g.,  $B' \equiv dB/dz$ ). Equations (A5)–(A8) are the linearized equations of continuity (combined with the induction equation), motion in the vertical direction, energy (for an adiabatic medium), and horizontal pressure balance, respectively. The perturbed quantities can be expressed in terms of  $\xi_{\parallel}$  through the relations (Hasan 1997)

$$\frac{\delta p}{p} = \frac{1}{2 + \beta} \left[ -2\gamma \frac{d\xi_{\parallel}}{dz} + \frac{\gamma g}{c_s^2} (2 - \gamma) \xi_{\parallel} + \gamma(\beta + 1) \frac{\Pi_e}{p_e} \right], \quad (\text{A9})$$

$$\frac{\delta B_{\parallel}}{B} = \frac{1}{2 + \gamma\beta} \left[ (\beta + 1) \frac{\Pi_e}{p_e} + \gamma\beta \frac{d\xi_{\parallel}}{dz} - \frac{g}{c_s^2} \gamma\beta(2 - \gamma) \xi_{\parallel} \right]. \quad (\text{A10})$$

Substituting equations (A9) and (A10) into equation (A6) and using equation (A7) to eliminate  $\delta\rho$ , we arrive at the following equation (valid for an isothermal medium) in terms of  $\xi_{\parallel}$ :

$$\frac{\partial^2 \xi_{\parallel}}{\partial z^2} - \frac{1}{2H} \frac{\partial \xi_{\parallel}}{\partial z} - \frac{1}{c_{\lambda}^2} \frac{\partial^2 \xi_{\parallel}}{\partial t^2} - \frac{1}{2H^2} \frac{\gamma - 1}{\gamma} (1 + \beta) \xi_{\parallel} = \frac{1 + \beta}{2p_e} \left( \frac{d}{dz} + \frac{1}{\gamma H} \right) \Pi_e. \quad (\text{A11})$$

We now define a new variable  $Q_{\lambda}$  through

$$\xi_{\parallel} = e^{z/4H} Q_{\lambda}. \quad (\text{A12})$$

Making the above substitution in equation (A11), we obtain

$$\frac{\partial^2 Q_{\lambda}}{\partial z^2} - \frac{1}{c_{\lambda}^2} \frac{\partial^2 Q_{\lambda}}{\partial t^2} - k_{\lambda}^2 Q_{\lambda} = e^{-z/4H} \frac{\beta + 1}{2p_e} \left( d dz + \frac{1}{\gamma H} \right) \Pi_e, \quad (\text{A13})$$

where

$$k_{\lambda}^2 = \frac{1}{H^2} \left[ \frac{\gamma - 1}{\gamma^2} \left( 1 + \frac{\gamma\beta}{2} \right) + \left( \frac{3}{4} - \frac{1}{\gamma} \right)^2 \right].$$

Equation (A13), without the inhomogeneous term on the right-hand side, was derived by Rae & Roberts (1982).

## APPENDIX B

## EXCITATION OF KINK WAVES BY FOOTPOINT MOTIONS

We develop the solution in terms of  $\dot{Q}_\kappa$ , which satisfies the homogeneous Klein-Gordon equation for a semi-infinite medium extending from  $z = 0$  to  $z = \infty$ :

$$\frac{\partial^2 \dot{Q}_\kappa}{\partial z^2} - \frac{1}{c_\kappa^2} \frac{\partial^2 \dot{Q}_\kappa}{\partial t^2} - k_\kappa^2 \dot{Q}_\kappa = 0, \quad (\text{B1})$$

subject to an inhomogeneous boundary condition at  $z = 0$ , where  $\dot{Q}_\kappa$  is specified as a function of time. The solution of equation (B1) can be determined using a Green's function technique. The Green's function for this problem that vanishes at  $z = 0$  can be constructed in terms of the corresponding function for an infinite medium (given by eq. [10]), which is

$$G_\kappa(z, z_0; t, t_0) = \frac{c_\kappa}{2} \left\{ J_0 \left[ \omega_\kappa \sqrt{(t-t_0)^2 - \frac{(z-z_0)^2}{c_\kappa^2}} \right] \mathcal{H} \left( t-t_0 - \frac{z-z_0}{c_\kappa} \right) - J_0 \left[ \omega_\kappa \sqrt{(t-t_0)^2 - \frac{(z+z_0)^2}{c_\kappa^2}} \right] \mathcal{H} \left( t-t_0 - \frac{z+z_0}{c_\kappa} \right) \right\}. \quad (\text{B2})$$

The above equation follows by superposing the Green's functions of two sources at  $z = z_0$  and  $z = -z_0$ , respectively. The solution of equation (B1) in terms of  $G_\kappa$  given by equation (B2) is

$$\dot{Q}_\kappa(z, t) = \int_0^t dt_0 \dot{Q}_\kappa(0, t_0) \left. \frac{\partial G_\kappa}{\partial z_0} \right|_{z_0=0}. \quad (\text{B3})$$

Substituting

$$\left. \frac{\partial G_\kappa}{\partial z_0} \right|_{z_0=0} = \delta \left( t-t_0 - \frac{z}{c_\kappa} \right) - \frac{k_\kappa z}{\sqrt{(t-t_0)^2 - (z/c_\kappa)^2}} J_1 \left[ \omega_\kappa \sqrt{(t-t_0)^2 - \left( \frac{z}{c_\kappa} \right)^2} \right] \mathcal{H} \left( t-t_0 - \frac{z}{c_\kappa} \right) \quad (\text{B4})$$

in equation (B3), yields the desired result, viz.,

$$\dot{Q}_\kappa(z, t) = \dot{Q}_\kappa \left( 0, t - \frac{z}{c_\kappa} \right) - k_\kappa z \int_0^{t-z/c_\kappa} dt_0 \dot{Q}_\kappa(0, t_0) \frac{J_1(\omega_\kappa \zeta_\kappa)}{\zeta_\kappa}, \quad (\text{B5})$$

where

$$\zeta_\kappa = \sqrt{(t-t_0)^2 - (z/c_\kappa)^2}.$$

## REFERENCES

- Berger, T. E., Löfdahl, M. G., Shine, R. A., & Title, A. M. 1998, *ApJ*, 506, 439  
 Berger, T. E., Schrijver, C. J., Shine, R. A., Tarbell, T. D., Title, A. M., & Scharmer, G. 1995, *ApJ*, 454, 531  
 Bogdan, T. J. 1992, NATO ASI Series C, ed. J. H. Thomas & N. O. Weiss (Dordrecht: Kluwer), 375, 345  
 ———. 1994, in *Solar Magnetic Fields*, ed. M. Schüssler & W. Schmidt (Cambridge: Cambridge Univ. Press), 229  
 Bogdan, T. J., Hindman, B., Cally, P. S., & Charbonneau, P. 1996, *ApJ*, 465, 406  
 Bogdan, T. J., & Zweibel, E. G. 1985, *ApJ*, 298, 867  
 Brandt, P. N., Rutten, R. J., Shine, R. A., & Trujillo Bueno, J. 1992, in *ASP Conf. Ser. 26, Cambridge Workshop on Cool Stars, Stellar Systems, and the Sun*, ed. M. S. Giampapa & J. A. Bookbinder (San Francisco: ASP), 161  
 Bray, R. J., & Loughhead, R. E. 1974, *The Solar Chromosphere* (London: Chapman and Hall), chap. 6  
 Choudhuri, A. R., Auffret, H., & Priest, E. R. 1993, *Sol. Phys.*, 143, 49 (CAP93)  
 Choudhuri, A. R., Dikpati, M., & Banerjee, D. 1993, *ApJ*, 413, 811  
 Curdt, W., & Heinzel, P. 1998, *ApJ*, 503, L95  
 Damé, L. 1983, Thèse, Université de Paris VII  
 Deubner, F. L., & Fleck, B. 1990, *A&A*, 228, 506  
 Doetsch, G. 1956, *Handbuch der Laplace-Transformationen* (Basel: Birkhäuser)  
 Dunn, R. B., & Zirker, J. B. 1973, *Sol. Phys.*, 33, 281  
 Hasan, S. S. 1997, *ApJ*, 480, 803  
 Hasan, S. S., Kneer, F., & Kalkofen, W. 1998, *A&A*, 332, 1064  
 Huang, P., Musielak, Z. E., & Ulmschneider, P. 1995, *A&A*, 279, 579  
 Kalkofen, W. 1996, *ApJ*, 468, L69  
 Kalkofen, W. 1997, *ApJ*, 486, L145 (K97)  
 Kalkofen, W., Rossi, P., Bodo, G., & Massaglia, S. 1994, *A&A*, 284, 976  
 Keller, C. U., Deubner, F.-L., Egger, U., Fleck, B., & Povel, H. P. 1994, *A&A*, 286, 626  
 Kneer, F., Hasan, S. S., & Kalkofen, W. 1996, *A&A*, 305, 660  
 Lites, B. W., Rutten, R. J., & Kalkofen, W. 1993, *ApJ*, 414, 345 (LRK93)  
 Lou, Y. Q. 1995a, *MNRAS*, 274, L1  
 ———. 1995b, *MNRAS*, 276, 769  
 Mehlretter, J. B. 1974, *Sol. Phys.*, 38, 43  
 Morse, P. M., & Feshbach, H. 1953, *Methods of Theoretical Physics, Part I* (Kogakusha, Tokyo: McGraw-Hill), chap. 7  
 Muller, R. 1983, *Sol. Phys.*, 85, 113  
 ———. 1985, *Sol. Phys.*, 100, 237  
 Muller, R., & Roudier, Th. 1992, *Sol. Phys.*, 141, 27  
 Muller, R., Roudier, Th., Vigneanu, J., & Auffret, H. 1992, in *IAU Symp. 138, Solar Photosphere: Structure, Convection and Magnetic Fields*, ed. J. O. Stenflo (Dordrecht: Kluwer), 85  
 ———. 1994, *A&A*, 283, 232  
 Musielak, Z. E., Rosner, R., Gail, H. P., & Ulmschneider, P. 1995, *ApJ*, 448, 865  
 Musielak, Z. E., Rosner, R., Stein, R. F., & Ulmschneider, P. 1994, *ApJ*, 423, 474  
 Nindos, A., & Zirin, H. 1998, *Sol. Phys.*, 179, 253  
 Nordlund, Å., Brandenburg, A., Jennings, R. L., Rieutord, M., Ruokainen, J., Stein, R. F., & Tuominen, I. 1992, *ApJ*, 392, 647  
 Nordlund, Å., & Stein, R. F. 1989, in *NATO ASI Series 263, Solar and Stellar Granulation*, ed. R. J. Rutten & G. Severino (Dordrecht: Kluwer), 453  
 ———. 1990, in *IAU Symp. 138, Solar Photosphere: Structure, Convection and Magnetic Fields*, ed. J. O. Stenflo (Dordrecht: Kluwer), 191

- Rae, I. C., & Roberts, B. 1982, *ApJ*, 256, 761
- Roberts, B., & Webb, A. R. 1978, *Sol. Phys.*, 56, 5
- Rüedi, I., Solanki, S. K., Livingston, W. C., & Stenflo, J. O. 1992, *A&A*, 263, 323
- Ryutov, D. A., & Ryutova, M. P. 1976, *Soviet Phys.-JETP*, 43(3), 491
- Ryutova, M. P., & Priest, E. R. 1993, *ApJ*, 419, 349
- Sivaraman, K. R., & Livingston, W. C. 1982, *Sol. Phys.*, 80, 227
- Spruit, H. C. 1981, *A&A*, 98, 155
- . 1982, *Sol. Phys.*, 75, 3
- Spruit, H. C., & Roberts, H. 1983, *Nature*, 304, 401
- Stein, R. F., Brandenburg, A., & Nordlund, Å. 1992, in *ASP Conf. Ser. 26, Stellar Systems and the Sun*, ed. M. Giampapa & J. Boobkinder (San Francisco: ASP), 148
- Steiner, O., Grossmann-Doerth, U., Knölker, M., & Schüssler, M. 1998, *ApJ*, 495, 468
- Stenflo, J. O. 1994, *Solar Magnetic Fields* (Dordrecht: Kluwer)
- Tarbell, T. D., Ferguson, S., Frank, Z., Shine, R. A., Title, A. M., Topka, K. P., & Scharmer, G. 1989, in *IAU Symp. 138, Solar Photosphere: Structure, Convection and Magnetic Fields*, ed. J. O. Stenflo (Dordrecht: Kluwer), 147
- Title, A. M., Topka, K. P., Tarbell, T. D., Schmidt, W., Balke, C., & Scharmer, G. 1992, *ApJ*, 393, 782
- Ulmschneider, P. 1970, *Sol. Phys.*, 12, 403
- Ulmschneider, P., Zähringer, K., & Musielak, Z. E. 1991, *A&A*, 241, 625
- van Ballegooijen, A., Nissenson, P., Noyes, R. W., Löfdahl, M. G., Stein, R. F., Nordlund, Å., & Krishnakumar, V. 1998, *ApJ*, 509, 435
- Wang, J., Wang, H., Lee, J. W., & Zirin, H. 1995, *Sol. Phys.*, 160, 277
- Withbroe, G. W. 1988, *ApJ*, 325, 442
- Zhugzhda, Y. D., Bromm, V., & Ulmschneider, P. 1995, *A&A*, 300, 302
- Zweibel, E. G., & Bogdan, T. J. 1986, *ApJ*, 308, 401